Veterinary Parasitology 345 (2026) 110797

Contents lists available at ScienceDirect

Veterinary Parasitology

journal homepage: www.elsevier.com/locate/vetpar

Comparative ex vivo responses of ovine and bovine polymorphonuclear neutrophils induced by *Neospora caninum* tachyzoites

D. Gutiérrez-Expósito [a,b,*], L.M. R. Silva [a,c,d], H. Wagner [e], U. Gärtner [f], C. Hermosilla [a], A. Taubert [a], Conejeros I [a]

[a] Institute of Parasitology. Justus Liebig University Giessen, Giessen, Germany
[b] Grupo SANPATRUM. Departamento de Sanidad Animal, Facultad de Veterinaria, Universidad de León. Campus Vegazana, León, Instituto de Ganadería de Montaña (IGM-CSIC), España
[c] Egas Moniz Center for Interdisciplinary Research (CiiEM), Egas Moniz School of Health & Science, Caparica, Portugal
[d] Laboratory of Parasitology, National Institute for Agrarian and Veterinary Research, IP, Oeiras, Portugal
[e] Veterinary Clinic for Reproductive Medicine and Neonatology, Justus Liebig University Giessen, Giessen, Germany
[f] Institute of Anatomy and Cell Biology, Justus Liebig University Giessen, Giessen, Germany

ARTICLE INFO

Keywords:
NETs formation
ROS
Innate immune response
Neospora caninum
Cattle
Sheep

ABSTRACT

Neospora caninum infection causes reproductive failure in ruminants with a traditionally higher incidence of bovine neosporosis compared to the ovine system. Differences in innate immune response could explain this observation. We here focused our study on the comparison of the *N. caninum*-induced response on bovine and ovine polymorphonuclear neutrophils (PMN) that might play a key role in the pathogenesis of neosporosis in both small and large ruminants. We here examined and compared in parallel PMN responses of healthy adult sheep ($n = 6$) and cows ($n = 6$) after exposure to *N. caninum* tachyzoites (ratio 1:4). PMN activation was evaluated by induction of NETosis, determined by immunofluorescence and scanning electron microscopy (SEM), extracellular reactive oxygen species (ROS) production via Amplex Red assays, and oxygen consumption rates (OCR) and proton efflux rates (PER) quantified by Seahorse XF technology. *N. caninum* tachyzoite-driven percentage of NETotic PMN was higher in the bovine system (24.4%) when compared to sheep (11.3%). For both, SEM analyses confirmed PMN activation and the formation of NET structures upon *N. caninum* tachyzoite exposure. The increase in tachyzoite-mediated ROS production proved higher in cattle than in sheep and these data were in line with significantly higher PER on bovine PMN indicating a differential glycolytic activity upon *N. caninum* exposure. Overall, this study documents early (minutes) and mid-late (hours) ovine and bovine PMN reactions after being exposed to *N. caninum* tachyzoites. The fundamental information here given contributes to the understanding of neosporosis in cows and sheep that should be complemented with *in vivo* studies.

1. Introduction

Neospora caninum is an obligate intracellular apicomplexan parasite which infects wild and domestic ruminants, causing significant economic losses worldwide due to reproductive disorders, mainly in cattle, one of the most sensitive hosts (Dubey et al., 2007). However, over the last three decades, ovine neosporosis is gaining importance and seems to be more prevalent than previously expected. It remains unclear why the incidence of neosporosis in bovines is traditionally higher than in sheep, despite similar clinical signs and lesions (Benavides et al., 2022, Mendoza-Morales et al., 2022). The precise mechanisms by which *N. caninum*-induced inflammatory responses damage placenta and fetus, often leading to organ failure and abortion, remain unclear. In this sense, any leukocyte population of the host innate immune system, such as polymorphonuclear neutrophils (PMN) (Villagra-Blanco et al., 2017a, Villagra-Blanco et al., 2017b), NK cells (Boysen et al., 2006; García--Sanchez et al., 2021) or monocytes (Sharma et al., 2018), might play a key role in the pathogenesis of ruminant neosporosis or may be critical for the outcome of *N. caninum* infection (Taubert et al., 2006; Hermosilla et al., 2014; García-Sánchez et al., 2021). However, the precise role of ruminant PMN during vertical transmission and subsequent abortions after primary infections as well as after recrudescence in chronically

* Corresponding author at: Grupo SANPATRUM. Departamento de Sanidad Animal, Facultad de Veterinaria, Universidad de León. Campus Vegazana S/N, 24071. Instituto de Ganadería de Montaña CSIC-ULE, León, España.
E-mail address: dgute@unileon.es (D. Gutiérrez-Expósito).

https://doi.org/10.1016/j.vetpar.2026.110797
Received 27 March 2026; Received in revised form 27 April 2026; Accepted 9 May 2026
Available online 13 May 2026
0304-4017/© 2026 The Author(s). Published by Elsevier B.V. This is an open access article under the CC BY-NC-ND license (http://creativecommons.org/licenses/by-nc-nd/4.0/).

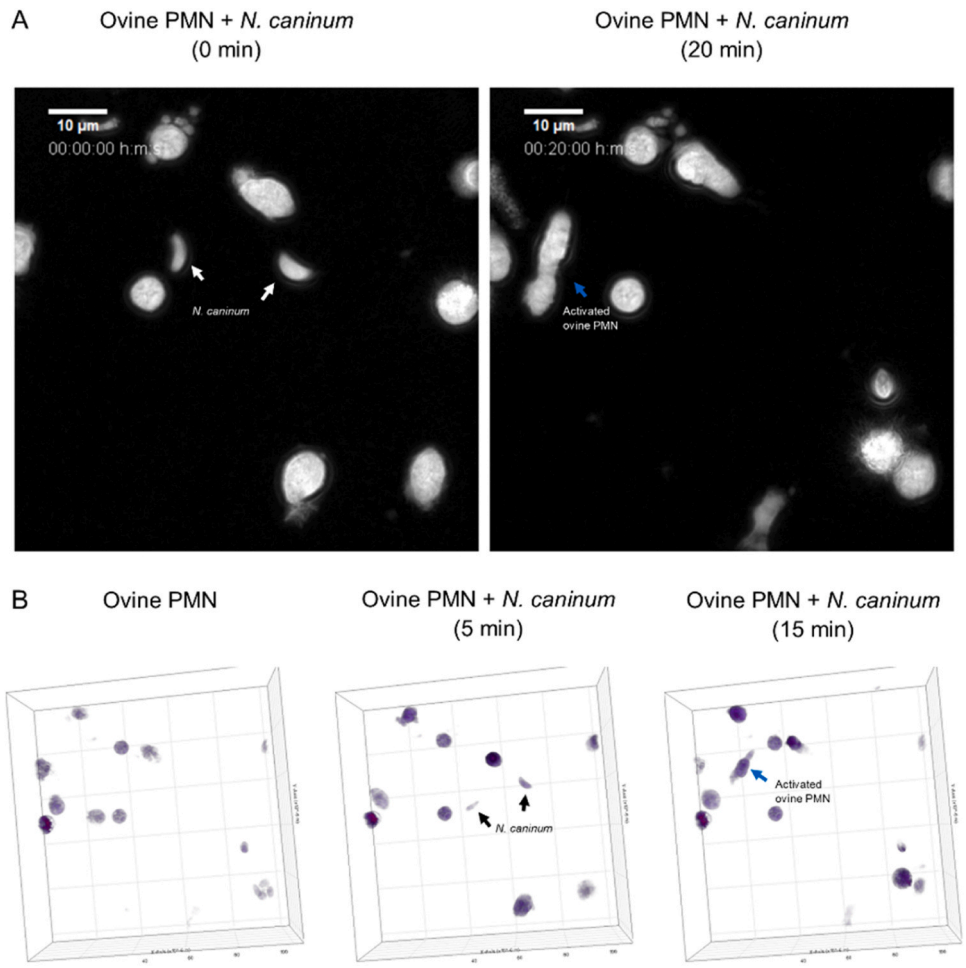

Fig. 1. and supplementary video 1. Live-cell 3D-holotomographic microscopy of ovine PMN co-incubated with *N. caninum*. (A) Refractive index (RI)- based images of ovine PMN exposed to *N. caninum* tachyzoites at time 0 min (control) and after 20 min of interaction. (B) RI-based digital staining of ovine PMN exposed to *N. caninum* tachyzoites for 0,5 and 20 min. White and black arrows indicate *N. caninum* tachyzoites. Blue arrows indicate activated ovine PMN.

infected pregnant cattle and sheep during successive pregnancies is still unknown (Buxton et al., 2002; González-Warleta et al., 2018).

PMN are recruited and activated into bovine/ovine female reproduction tract during pregnancy and in bacterial infection events (Bondurant, 1999; Gilbert et al., 2005). Furthermore, PMN were demonstrated to inhibit apicomplexan host cell invasion (Behrendt et al., 2010; Muñoz-Caro et al., 2015; Villagra-Blanco et al., 2017a) and to control parasite replication (Bliss et al., 2001; Mohammed et al., 2022). PMN can kill invading pathogens by several effector mechanisms, such as phagocytosis, the generation of reactive oxygen species (ROS), degranulation, the release of neutrophil extracellular traps (NETs) and swarming (Lee et al., 2003; Brinkmann et al., 2004; Lacy, 2006; Brown and Yipp, 2023). PMN-derived defense mechanisms have been extensively studied in humans and mice not only *ex vivo* (Castanheira and Kubes, 2019; Nauseef, 2023) but also *in vivo* (Brinkmann et al., 2016; Klinke et al., 2023). However, respective knowledge in ruminants is still limited (Muñoz-Caro et al., 2016; Worku et al., 2021). Nevertheless, several studies already confirmed different *ex vivo* functions of ruminant PMN (mainly cattle) against bacteria (i.e. *Mycobacterium avium* subsp *paratuberculosis*) and apicomplexan parasites (i.e. *Eimeria bovis*, *E. arloingi*, *Cryptosporidium parvum*, *Besnoitia besnoiti*, *Toxoplasma gondii* and *N. caninum*) (Behrendt et al., 2010; Muñoz-Caro et al., 2015a, 2016; Silva et al., 2014; Ladero-Auñon et al., 2021; Zhang et al., 2021; Hasheminasab et al., 2022).

One of the most studied effector mechanisms under *ex vivo* conditions of ruminant PMN against apicomplexans is the formation of NETs. *N. caninum*-induced NETosis in cattle and goats is parasite dose- and time-dependent (Villagra-Blanco et al., 2017a, Villagra-Blanco et al., 2017b). To date, no data is available on *N. caninum*-induced NETosis in sheep. *N. caninum*-induced NETosis also proved to depend on $Ca^{+\,+}$ influx and on purinergic signaling in PMN since both the inhibition of store-operated calcium entry (SOCE) and of purinergic receptor P2Y2-mediated ATP uptake diminished NET formation (Villagra-Blanco et al., 2017a). Another important PMN effector mechanism, ROS production, is also activated upon exposure to protozoan parasites (Silva et al., 2014; Zamboni and Lima-Junior, 2015; Grob et al., 2020). This event proved to be essential for most types of NET release (Hakkim et al., 2011; Almyroudis et al., 2013, Fonseca et al., 2018). Also, parasite-induced NET formation depends on calcium influx, ERK1/2-, MAPK p38-, PI3K/Akt/HIF-1-mediated signaling and mitochondrial ROS ($_{mt}$ROS) production (Muñoz-Caro et al., 2015a, b; Villagra-Blanco et al., 2017a; Ravindran et al., 2019). These processes are linked to both, an increase in oxygen consumption rate (OCR) and an enhancement of proton efflux rates (PER) which also modulates NET formation (Chacko et al., 2013; Grob et al., 2020; Conejeros et al., 2022; Espinosa et al., 2023).

NETs have been characterized in several ruminant species such as cattle, sheep and goats (Worku et al., 2021); and, referring to apicomplexan parasites, differential host susceptibility and immune reactions were already reported in case of *T. gondii*-exposed ovine and bovine PMN (Yildiz et al., 2017). Whilst *T. gondii*-triggered ovine NETs caused mechanical immobilization of tachyzoites, bovine NETs also had direct

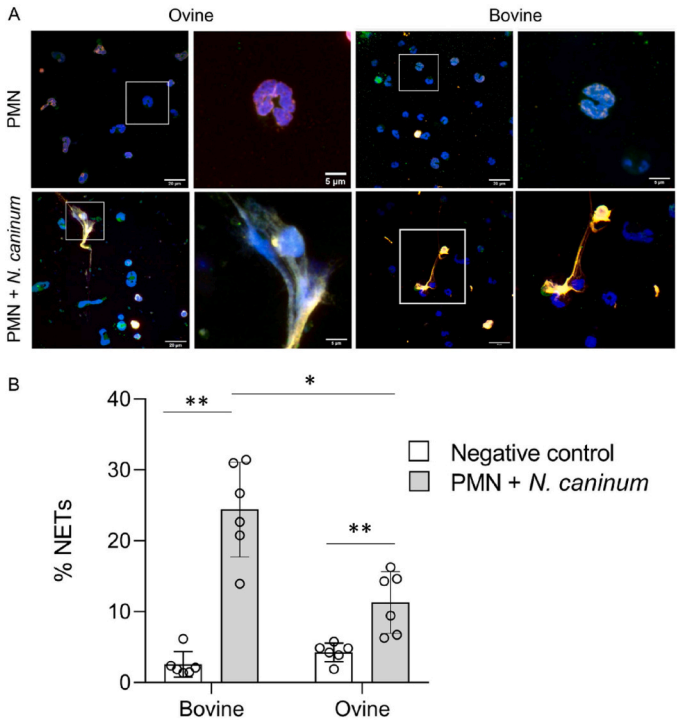

Fig. 2. *N. caninum* induces more NETs in bovine than ovine PMN. (A) Confocal microscopy analysis of non-exposed ovine and bovine PMN (2 ×105; control, added media only; upper panel) and *N. caninum*-exposed PMN (lower panel, *N. caninum* added at 1:4 ratio). Confocal microscopy analysis shows co-localization of DNA (blue), neutrophil elastase (NE) (green) and pan-histones (H1, H2A/H2B, H3, H4) (red). All images correspond to the merge of the three channels. White squares indicate the region of the image zoomed in the corresponding right panel. **(B)** Percentage of PMN that formed NETs out of the total. The number of NET-forming positive bovine PMN is higher than ovine PMN. Bars represent means of 6 animals with error bars representing the standard deviation. *P*-value was estimated by ANOVA test. ** $P < 0.05$, *** $P < 0.001$.

lethal effects on tachyzoites (Yildiz et al., 2017). The authors speculated that detrimental effects over *T. gondii* induced by bovine PMN might be driven by PMN-derived MPO. These effector mechanism-based differences may contribute to the phenomenon that *T. gondii*-infected cattle are less prone to abort than sheep (Dubey, 1986, Innes et al., 2007) leading us to hypothesize that differences in bovine and ovine PMN-mediated immune reactions might also be key for the different susceptibility of both ruminant species to *N. caninum* infection.

Thus, the aim of this study was to directly compare *ex vivo* immune response of PMN from sheep and cattle against *N. caninum* tachyzoites under the same experimental conditions (i.e. on the same *N. caninum* strain and PMN isolated on the same day to guarantee that the experiments were run in parallel) to enhance comprehension of the variances in the innate immunity and pathogenesis of neosporosis among large and small ruminants.

2. Material and methods

2.1. Animals

This study was carried out using healthy, adult, non-pregnant sheep ($n = 6$) (4–6 years-old) and cows ($n = 6$) (Rhönschaf and Holstein Friesian breed, respectively) (3–5 years-old) housed in the large animal facilities of the Veterinary Clinic for Reproductive Medicine and Neonatology, Justus Liebig University Giessen (JLU), Giessen, Germany. All animals were seronegative through commercial ELISA tests against different abortifacient agents of sheep (*T. gondii*, *N. caninum*, border disease virus, Schmallenberg virus, *Brucella* spp, *Coxiella burnetii*, and *Chlamydia abortus*) and cattle (*N. caninum*, Schmallenberg virus, *Brucella* spp, *Coxiella burnetii*, and *Chlamydia abortus*) before sampling. Included animal donors were under any specific sanitary plan and vaccinated against the following agents: i) ovines against *Clostridium* and ii) cattle against flu complex. Individual blood samples (30 mL) were collected twice a month to reduce stress and to allow fast recovery.

This study was conducted in accordance with the Justus Liebig University Giessen (JLU) Animal Care Committee Guidelines. Protocols for bovine blood sampling were approved by Ethic Commission for Experimental Animal Studies of Federal State of Hesse (Regierungspräsidium Giessen; A9/2012; JLU-No.521_AZ) and protocols for ovine blood sampling were also approved (Regierungspräsidium Giessen: Gi20/28 Nr. G2–2022; JLU-No. 1067_GP) as a part of another animal experiment.

2.2. Isolation of bovine and ovine PMN

Blood samples were collected by jugular venipuncture using 10 mL BD Vacutainer™ tubes with lithium heparin as anticoagulant. Isolation of ovine and bovine PMN was carried out simultaneously within 2 h after sampling as previously described with few modifications (Villagra-Blanco et al., 2017a). Briefly, 20 mL heparinized blood were re-suspended in sterile 20 mL PBS with 0.02% EDTA, layered on the top of 12 mL Histopaque®-1077 (Sigma-Aldrich) and centrifuged at room temperature (800 x *g*, 45 min). Afterwards, the red blood cell layer, located underneath the peripheral blood mononuclear cell (PBMC) layer and the plasma, was collected, diluted in Hank's balanced salt solution (HBSS) 1X up to 10 mL and mixed with 20 mL of ice-cold phosphate--based erythrocyte lysis buffer (5.5 mM NaH_2PO_4, 8.4 mM HK_2PO_4, pH 7.2) for 1 min. To restore the osmolarity, 10 mL of hypertonic buffer (5.5 mM NaH_2PO_4, 8.4 mM HK_2PO_4, 0.46 M NaCl, pH 7.2) were added and the total volume was adjusted to 50 mL with HBSS 1X. The erythrocyte lysis step was repeated once and PMN were washed in sterile HBSS 1X (600 x *g*; 6 min; 4 ºC). PMN were counted in a Neubauer chamber. The purity (> 90%) of the isolated PMN was assessed by direct microscopic visual evaluation by Diff-Quick staining whereas cell viability (> 87%) was determined by trypan blue 0.05% exclusion (Arteche-Villasol et al., 2022).

2.3. Parasites

Neospora caninum (Nc1 strain) (Dubey et al., 1988) tachyzoites were routinely cultivated *in vitro* in permanent African green monkey kidney epithelial cells (MARC-145) as previously described (Regidor-Cerrillo et al., 2008). When passaging, the cell layers were scraped-off, passed through a 25 G needle, and supplemented to non-infected cell layers. *N. caninum* tachyzoites were collected in supernatants from 3 to 3.5 days p. i., filtered (5 µm filter; Whatman®) and pelleted (400 x *g*, 15 min). Later, tachyzoites were counted in a Neubauer chamber, suspended in specific medium for each assay and used for PMN confrontation within 1 h after isolation. The viability of *N. caninum* tachyzoites (> 90%) was determined by trypan blue (0.05%) exclusion. All experiments were performed at a multiplicity of infection (MOI) of 1:4 (PMN:parasites) and duplicates were included in each experiment. A total of three independent experimental replicates per species were carried out for NET formation, ROS production and Seahorse experiments. In the case of 3D holotomographic microscopy (Nanolive) and scanning electron microscopy (SEM), the biological replicates were two.

2.4. Visualization of ovine PMN and N. caninum interaction by 3D holotomographic microscopy (Nanolive)

To study early ovine PMN-*N. caninum* interactions, a live-cell 3D holotomographic video was produced. A total of 5×10^5 ovine PMN were seeded into 35 mm low wall tissue culture µ-dish (Ibidi) in imaging

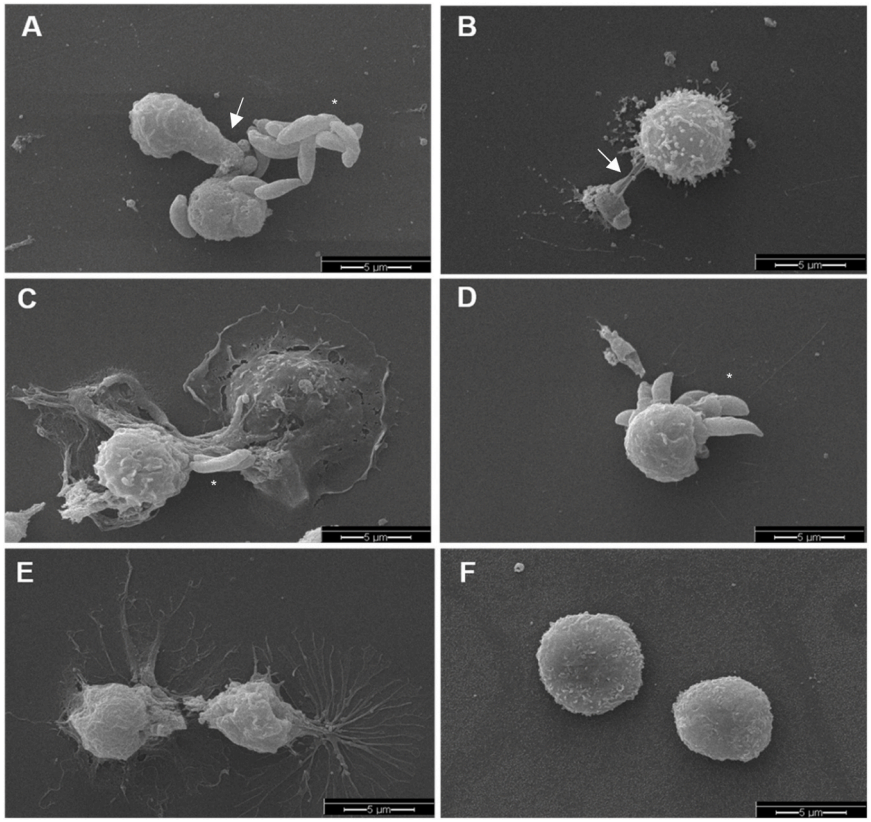

Fig. 3. *N. caninum* activates bovine and ovine PMN. Ovine PMN (A, B) and bovine PMN (C, D) were exposed to *N. caninum* tachyzoitzes for 3 h, fixed and analyzed by scanning electron microscopy (SEM). Some of the PMN-activation observed structures as pseudopodal extension in A and PMN-derived filaroid structure in B are highlighted with white arrows. An event of phagocytosis or active invasion is shown in D. *N. caninum* tachyzoites are indicated by an asterisk. E. Activation of bovine PMN stimulated with PMA. F. Non-stimulated and inactivated ovine PMNs.

medium [RPMI 1640 lacking phenol red and serum, supplemented with 0.5 μM Sytox Green (Life Technologies) and 2 μM DRAQ 5 (Thermo Scientific)]. After 30 min of incubation in an Oko-lab stage top incubation system at 37°C and 5% CO_2, *N. caninum* tachyzoites were added (1:3, 1.5×10^6). Then, holotomographic images were obtained by using a 3D cell-explorer microscope (Nanolive 3D) equipped with a 60x magnification ($\lambda = 520$ nm, sample exposure 0.2 mW/mm2) and a depth of field of 30 μm. DAPI channel (blue) was used to visualize DNA. Postprocessing and digital reconstruction of the sequence of images (1 frame every 30 s) of interaction during 4 h of experimentation was performed using Steve software (Nanolive). Merge of the image sequence and exporting to TIFF and mp4 data files was performed in Image J, Fiji Version (Schindelin et al., 2012).

2.5. Visualization and quantification of NETs

Bovine ($n = 6$) and ovine ($n = 6$) PMN were re-suspended in medium RPMI 1640 without phenol red (Gibco®) and then confronted in duplicates with *N. caninum* tachyzoites. Phorbol myristate acetate (PMA; 100 nM, Sigma-Aldrich®) and PBS 1x were used for positive and negative controls, respectively. A total of 2×105 PMN were seeded on sterile round glass coverslips of 13 mm diameter (Thermo Fischer Scientific), pre-treated with 0.002% fibronectin in 24-well culture plates (Greiner®). PMN were allowed to settle for 30 min at 37 ºC and 5% CO_2 in a humidified incubator before exposure. After stimulant exposure, the cells were fixed in 4% paraformaldehyde (Merck®) for 15 min and stored at 4 ºC until use.

Visualization of NETs and of NET-specific components was performed by immunofluorescence assays detecting and co-localizing histones (mouse monoclonal anti-Pan-Histone-antibodies, 1:200, Merck #MAB3422) and neutrophil elastase (rabbit polyclonal NE, anti-NE-antibodies, 1:200, Abcam #ab68672). Therefore, fixed samples were washed three times with sterile PBS and blocked (60 min) in 3% bovine serum albumin (BSA; Sigma-Aldrich®) containing 0.3% Triton X-100 (Thermo Fischer Scientific®) and incubated with primary antibody solutions overnight at 4 ºC. Thereafter, three washing steps were performed with sterile PBS. Then, samples were incubated in secondary antibody solutions (Alexa Fluor 594 goat anti-mouse IgG #A11005, Alexa Fluor 488 goat anti-rabbit IgG #A11008, 1:500, Invitrogen) for 30 min at room temperature (RT) in complete darkness. Finally, the samples were washed three times with sterile PBS and mounted upside-down with Fluoromount-G™ Mounting Medium with 4′,6-diamidino-2-phenylindole (DAPI) at RT. Visualization of NET formation was achieved using an inverted IX81® epifluorescence microscope equipped with an XM 10® digital camera (both Olympus) and by applying confocal microscopy (Zeiss LSM 710®).

The percentage of PMN releasing NETs was calculated in immunostained samples by epifluorescence microscopic analysis based on 5 pictures randomly taken from each experimental condition (520 PMN/picture on average) using ImageJ® software as previously described (Brinkmann et al., 2013).

For the study of NETs component co-localization, images were acquired with a Zeiss Confocal LSM 710 equipped with a motorized XY stage and oil 63x objective (numerical aperture of 1.4) or by a Nikon Eclipse Ti2-A inverted microscope equipped with a ReScan confocal microscope instrumentation (RCM 1.1 Visible, Confocal.nl) and a motorizes z-stage (DI1500). Three channels were recorded for signal detection: AlexaFluor594/Red/Hene-543 laser, AlexaFluor488/Green/Argon-laser and Blue/DAPI/405-laser. Images were acquired with a digital camera controlled by Zeiss ZEN 2010 software or using the NIS-

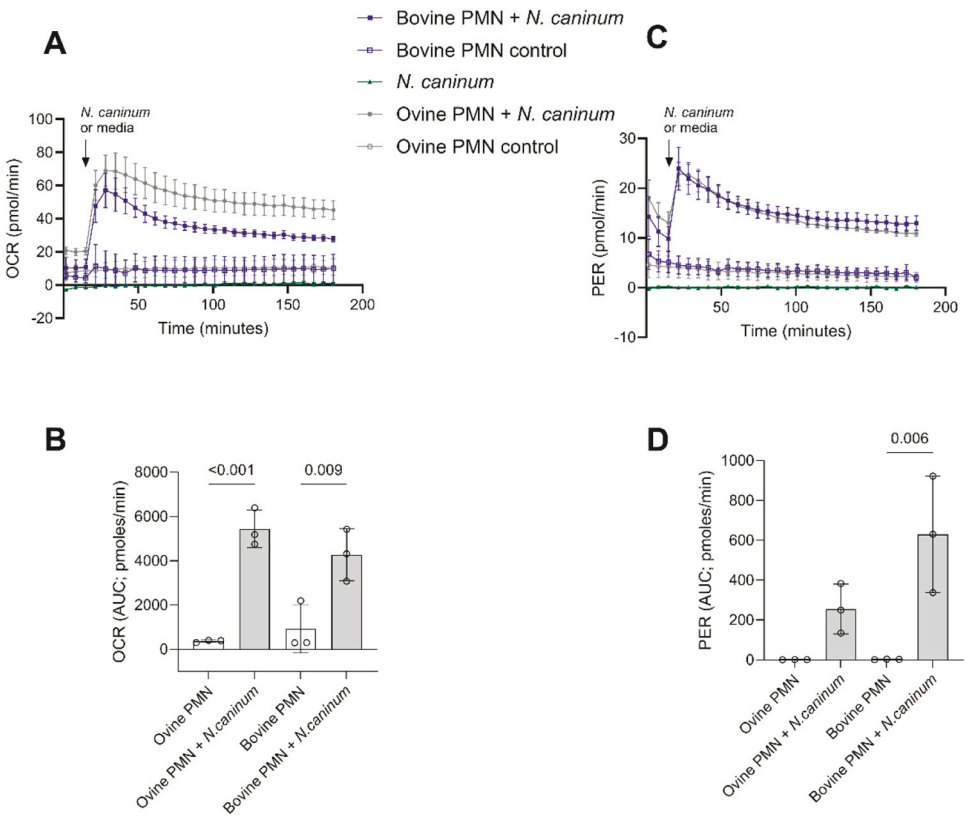

Fig. 4. *N. caninum* -induced oxidative and glycolytic response of bovine and ovine PMN. Oxygen consumption rate (A, B) and proton efflux rate (C, D) from ovine and bovine PMN were registered using an extracellular flux analyzer (Seahorse XFp) after *N. caninum* or media injection as negative control. B and D show the area under the curve (AUC) analyses for ovine and bovine PMN respectively. Bar plots represent mean ± SD ($n = 3$).

Elements v 5.11 software (Nikon). Samples were imaged by z-stack optical series with a step-size of 0.0–0.5 microns depth. The z-series were displayed as maximum z-projections, and gamma, brightness, and contrast were adjusted (identically for compared image sets) using Image J software, FIJI version (Schindelin et al., 2012).

2.6. Scanning electron microscopy (SEM)

Ovine and bovine PMN ($n = 3$) were co-cultured with *N. caninum*-tachyzoites (ratio 1:4) for 4 h on 10 mm Ø glass coverslips pre-coated with 0.01% poly-$_L$-lysine (Sigma-Aldrich) at 37 ºC and 5% CO_2. PMA (100 nM) and RPMI 1640 were used as positive and negative controls, respectively, applying the same experimental conditions. Cells were fixed (1.5% glutaraldehyde/1.5% paraformaldehyde in HEPES-buffer 0.3 M), post-fixed in 1% osmium tetroxide (all Merck), washed in distilled water, dehydrated, critical point dried by CO_2-treatment and sputtered with gold particles. Finally, samples were visualized using a Philips XL30 scanning electron microscope at the Institute of Anatomy and Cell Biology, JLU Giessen, Germany.

2.7. Release of reactive oxygen species (ROS) by bovine and ovine PMN

The release of ROS (specifically, H_2O_2) by PMN of sheep ($n = 6$) and cattle ($n = 6$) was measured via Amplex Red® assays as previously described Rinaldi et al. (2007) with few modifications. Briefly, a total of 2 × 105 PMN/well in 100 µl of RPMI-1640 without phenol red (Gibco®) were seeded in a 96-well plate and mixed with 66.5 µl of pre-warmed Amplex Red reaction mixture [Amplex Red® 20 mM and horseradish peroxidase 20 U/mL diluted in RPMI-1640 without phenol red (Gibco®)]. To evaluate the effect of the ROS inhibitor diphenyleneiodonium chloride (DPI; 96 µM, Sigma-Aldrich), PMN were pre-incubated in 10 µl DPI (9,6 µM) for 10 min at 37 ºC. Parasites (8 ×105 tachyzoites), plain medium (negative control) or PMA (100 nM) (positive control) were added to PMN, and the sample volume was adjusted to 200 µl with RPMI. Fluorescence intensity was measured every 10 min in a Varioskan Flash plate reader (Thermo Fischer Scientific®) at an excitation wavelength of 530 nm and an emission wavelength of 590 nm. Background values, defined as the mean fluorescence intensity of plain Amplex Red® reaction mixture diluted in RPMI-1640 without phenol red (Gibco®) were subtracted from all readings. To calculate hydrogen peroxide concentrations, a standard curve on different H_2O_2 concentrations (1–6 µM, diluted in RPMI-1640 medium without phenol red) was included in each plate.

2.8. Quantification of oxygen consumption rates (OCR) and proton efflux rates (PER) in Neospora caninum-exposed PMN

Activation of bovine and ovine PMN was monitored using Seahorse XF analyzer (Agilent). Briefly, 1 × 106 PMN from each donor (sheep and cattle, each $n = 6$) were pelleted at 300 *g* for 10 min and resuspended in 250 µl of XF RPMI assay medium (Agilent) supplemented with 2 mM of $_L$-glutamine, 1 mM pyruvate and 10 mM glucose (all Agilent). A total of 50 µl of each cell solution corresponding to 2 × 105 cells were gently placed in each well of an eight-well XF analyzer plate (Agilent) pre-coated for 30 min with 0.001% poly-$_L$-lysine (Sigma-Aldrich). Then, 50 µl of XF assay medium (Agilent) was added to blank wells (no cell-controls), 130 µl of XF assay medium was added to each well and cells were incubated at 37 ºC without CO_2 for 45 min before measuring. *N. caninum* tachyzoites were resuspended in XF assay medium (8 ×105 parasites/20 µl) and added to PMN via instrument-own injection ports. For negative PMN controls, 20 µl of XF assay medium instead of *N. caninum* tachyzoites was used. Each sample was measured in duplicates. The monitoring phase included basal measurement of three readings followed by injection of tachyzoites or medium and 25

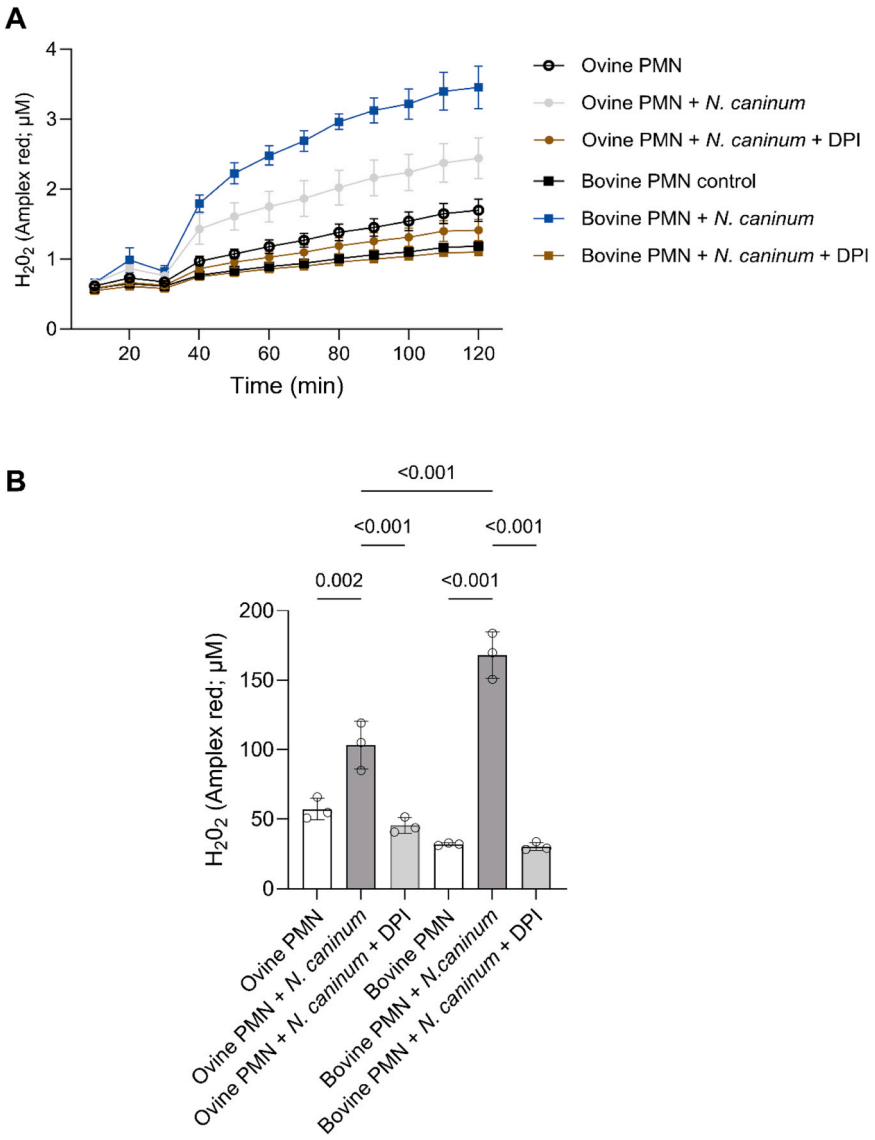

Fig. 5. *N. caninum* induces extracellular hydrogen peroxide production in bovine and ovine PMN. Ovine and bovine PMN (n = 6) were exposed to *N. caninum* tachyzoites (MOI 1:4) in the presence or absence of the NADPHOX inhibitor DPI. The ROS production detected by the Amplex Red reagent was measured every 10 min during 120 min of co-incubation (A). The bar plot in (B) shows the area under the curve (AUC) analysis of the obtained registries. Bars in the graph represents mean ± SD ($n = 3$).

consecutive readings. Background subtraction as well as determination of OCR and PER via obtained registries were performed using the Wave® software (Desktop Version, Agilent). The area under the curve of the obtained registries was determined using the software GraphPad Prism v. 10.6.1.

2.9. Statistical analysis

The data of the different parameters were analyzed according to the different ruminant species and stimuli, calculated using conventional descriptive statistical procedures and represented by bar and line plots. Shapiro-Wilk test was used to assess data normality. Parametric and non-parametric tests were used depending on the sample size, type of data and the variable to be analyzed. One- or two-factorial analyses of variance (ANOVA) were applied followed by a Tukey's range test to compare co-culture/stimulation conditions between both species using a normal distribution of data. The differences were considered as significant at a level of $*p \leq 0.05$; $** p \leq 0.01$ and $*** p \leq 0.001$, respectively. Statistical analyses were performed by GraphPad Prism® 8.0 software.

3. Results

3.1. N. caninum tachyzoites activates ovine PMN

Previously it was reported that bovine and goat PMN indeed are activated and form NETs upon exposure to *N. caninum* tachyzoites (Villagra-Blanco et al., 2017a, Villagra-Blanco et al., 2017b). We here recorded early activation of ovine PMN upon exposure to ovine PMN by live cell 3D holotomographic microscopy. Refractive index (RI) images (Fig. 1 A and supplementary video 1) and the RI-derived digital staining (Fig. 1B and supplementary video 2) show activation of ovine PMN upon *N. caninum* exposition as soon as 15 min.

Supplementary material related to this article can be found online at doi:10.1016/j.vetpar.2026.110797.

3.2. N. caninum tachyzoites induce a higher NET release in bovine than ovine PMN

NET formation of bovine and ovine PMN being confronted with

N. caninum tachyzoites was compared at 4 h of interaction by analyzing classical components of NETs by immunofluorescence microscopy. In both host systems, NET structures showed co-localization of extracellular chromatin, histones (H1, H2A/H2B, H3, H4) and NE (Fig. 2A) and typical NET-related characteristics, such as membrane-unbound and spread chromatin (Fig. 2A). Ovine and bovine PMN-derived NET structures were also observed after exposure to the chemical PKC activator PMA (Supplementary Fig 1). In non-stimulated controls, a low occurrence of NETs was observed, corresponding to spontaneous NETs.

The percentage of ovine and bovine PMN undergoing NETosis was analyzed and quantification of NET-positive cells revealed 24.4% of bovine PMN undergoing a NETotic process after exposure to *N. caninum* tachyzoites ($p < 0.001$) whilst the percentage in ovine PMN (11.3%) was lower ($p < 0.05$) (Fig. 2B). Interestingly, in the bovine system, the proportion of PMN performing *N. caninum* tachyzoite-driven was rather large since these values even exceeded the reactions driven by the potent stimulus PMA (12.8%). Overall, no statistical differences between both species were observed when PMN were stimulated with PMA stimulus ($p > 0.05$) Supplementary figure 1. As expected, stimulation with both *N. caninum* tachyzoites and PMA resulted in a statistically significant increase of NET release compared to negative controls ($p < 0.001$) (Supplementary figure 1).

In addition, SEM analysis confirmed the formation of a delicate network of thin strands of PMN-derived fibers being attached to *N. caninum* tachyzoites after 4 h of exposure entrapping some parasite stages whilst others were observed entrapped in chunky meshwork of PMN-derived filaments (Fig. 3). In addition, PMN activation was also observed as pseudopodia extension and eventual tachyzoite phagocytosis (Fig. 3). In positive controls the formation of thin strands of PMN-derived fibers were also detected, which were absent in negative controls (Fig. 3).

3.3. Bovine PMN show stronger oxidative and glycolytic responses after *N. caninum* tachyzoite exposure than ovine neutrophils

Activation of PMN exposed to *N. caninum* tachyzoites was also evaluated by the Seahorse technology, determining OCR and PER, reflecting neutrophil oxidative and glycolytic responses, respectively. After obtaining 3 basal readings (about 18 min) of OCR and PER in non-stimulated PMN, supplementation of live parasites resulted in a fast increase in OCR (4 fold) and PER (2,5 fold) in PMN from both ruminant species when compared to medium controls thereby indicating that PMN reacted by both oxidative and glycolytic responses (Figs. 4A and 4C). In the case of OCR, a slightly higher response was observed in *N. caninum*-confronted ovine PMN than *N. caninum*-confronted bovine PMN (Fig. 4B). In both cases, the increase in OCR was observed compared with control ovine ($p < 0.001$) and bovine ($p = 0.009$) PMN (Fig. 4B). Interestingly, *N. caninum*-exposed bovine PMN increased 3-fold more the PER than *N. caninum*-exposed ovine PMN, even if the difference was not statistically significant, probably due to the low sample size (Fig. 4D).

One of the main sources of oxygen consumption by PMN is the ROS production by NADPHOX, also referred as oxidative burst (Nauseef, 2007; Grudzinska et al. 2023). To evaluate if the observed enhanced parasite-driven OCR was linked to ROS production, extracellular H_2O_2 production was monitored for 120 min in *N. caninum* tachyzoite-exposed PMN (Fig. 5). *N. caninum* exposure indeed induced ROS production by ovine ($p = 0.009$) and bovine ($p < 0.001$) PMN (Fig. 5). The strongest H_2O_2 release was observed for *N. caninum*-exposed bovine PMN compared with *N. caninum*-exposed ovine PMN. ($p < 0.001$, Fig. 5B). In both host systems, it took around 30 min until H_2O_2 was increasingly released by parasite-stimulated PMN until the end of the observation period (Fig. 5A). As expected, in both host systems parasite-driven H_2O_2 release was almost entirely blocked by DPI pre-treatments of PMN and related values dropped to control level (DPI treatments: bovine: $p < 0.001$; ovine: $p < 0.001$). The addition of PMA (positive control) showed high levels of H_2O_2 after 30 min of incubation in both species ranging from 10.35 μM to 25.94 μM until the end of the experiment (120 min) ($p < 0.001$) Supplementary figure 1.

4. Discussion

Early innate host defense reactions have been identified as critical for the outcome of *N. caninum* infection in cattle, one of the most sensitive hosts (Boysen et al., 2006; García-Sánchez et al., 2021; Sharma et al., 2018). Hence, *N. caninum* was recently identified as a potent NET inducer *ex vivo* in ruminants like cattle and goats (Villagra-Blanco et al., 2017a, Villagra-Blanco et al., 2017b). However, to the best of our knowledge, in the current study we describe for the first time the release of ovine NETs in response to *N. caninum* tachyzoites. Despite of *N. caninum* infection has been traditionally reported in cattle, ovine neosporosis is being recognized as an abortive disease in sheep worldwide and assumed to be underdiagnosed in the field (Benavides et al., 2022; Mendoza-Morales et al., 2022). In this sense, this study contributes, from a comparative perspective to understand differences between cattle and sheep in terms of innate immune response.

Even though NET formation was first reported in human PMN over two decades ago (Brinkmann et al., 2004), still little is known on its role in parasitic diseases of ruminants. Nevertheless, several reports on NET extrusion (NETosis) against different protozoan parasites, such as *E. bovis, B. besnoiti*, *Plasmodium falciparum*, *T. b. brucei* and *T. gondii* (Baker et al., 2008; Behrendt et al., 2010; Abi Abdallah et al., 2012; Muñoz-Caro et al., 2016; Grob et al., 2020) including *N. caninum* (Villagra-Blanco et al., 2017a, Villagra-Blanco et al., 2017b; Demattio et al., 2023) were already published. In the current study we focused on comparative analyses on *N. caninum*-driven PMN activities in the bovine and ovine system.

To guarantee for reliable comparisons, we here simultaneously isolated ovine and bovine PMN and processed all laboratory techniques at the same time for both species. Time of exposure and parasite dose were earlier identified as important factors in the induction of NETs *ex vivo* (Behrendt et al., 2010; Muñoz-Caro et al., 2014). Based on recent *Neospora*-related work (Villagra-Blanco et al., 2017a, Villagra-Blanco et al., 2017b), we here focused on one MOI (1:4) and exposure time (4 h), which was equally applied for both host systems. Overall, immunofluorescence and SEM analyses confirmed the presence of DNA-rich structures forming extracellular networks with co-localization of NE and histones, i. e. classical characteristics of NETs, in both, ovine and bovine PMN. Interestingly, bovine PMN formed more NETs than ovine PMN. Given that suicidal NETosis requires PMN activation which in most cases rely on oxidative reactions (Huang et al., 2022), we furthermore compared metabolic responses of ovine and bovine PMN after *N. caninum* exposure. In general, PMN show a rather broad repertoire of biological responses, including ROS-dependent and -independent effector mechanisms, therefore PMN-derived reactions are always closely linked to cellular metabolism (Burgos et al., 2022; Conejeros et al., 2022). Moreover, PMN may show glycolytic responses upon activation, naturally associated with high ATP generation (Grudzinska et al., 2023; Conejeros et al., 2022; Quiroga et al., 2023). To monitor such reactions, we here applied the Seahorse technology which allows us to directly follow OCR as indicator of oxidative responses and extracellular acidification via PER as indicator of glycolytic responses. In line to NET-related results, glycolytic (PER) responses were here stated for both host origins, but were more pronounced in the bovine system. Due to the phagocytic capacity of PMN, their activation may also result in oxidative burst activities in which the oxygen is consumed to generate superoxide and other reactive oxygen species, being essential to NET formation and critical for effective antimicrobial immunity (Burgos et al., 2022; Conejeros et al., 2022). Therefore, we here also measured PMN-derive ROS production on the level of H_2O_2 release. In agreement to above mentioned OCR, we here also detected a parasite-triggered

increase in ROS production, with the highest values found for bovine PMN, complementing the results obtained by immunofluorescence. Referring to metabolic responses, these data are in principle in line with other studies on ruminant PMN co-cultured with other extra- and intracellular parasites, such as *T. b. brucei*, *E. bovis* and *B. besnoiti* applying the same methodology (Grob et al., 2020; Conejeros et al., 2022; Espinosa et al., 2023).

Of note, when parasite-induced NETosis or other innate effector functions are studied, the genetic background, host species, age, gender may influence these reactions (Swain et al., 2014; Muñoz-Caro et al., 2015a; Garza et al., 2018; Thiam et al., 2020). A recent review focusing on ruminant-derived NETosis (i. e. cattle, sheep and goats) emphasizes not only on species- but also breed-dependent differences (Worku at al., 2021). The authors stated species-specific responses to pathogens in relation to NET formation thereby contributing to the better understanding of the pivotal role of NETosis in pathophysiology and severity of several diseases of domestic ruminants, such as laminitis, ruminitis, endometritis and mastitis. However, based on availability, we restricted current analyses to only one breed of both sheep and cattle. Therefore, it cannot be excluded that other breeds may deliver different results.

Considering all parameters here studied, a stronger *ex vivo* immune response of bovine PMN was observed when compared to ovine reactions, which may suggest an *a priori* more effective response in the bovine system. However, it needs to be considered that, *in vivo*, NETs act as a double-edged sword due to their capability to trap and eliminate pathogens but also to exacerbate inflammation thereby eventually inducing pathogenicity by organ damage (Kaplan and Radic, 2012; Euler and Hoffmann, 2019). Thus, it is tempting to hypothesize that a more effective *ex vivo* response of bovine PMN may not only lead to improved *N. caninum* clearance but also to enhanced pathogenicity of infection. Obviously, *ex vivo* studies on single cell types cannot mimic the *in vivo* microenvironment being present in bloodstream and tissues but nevertheless deliver important data on potentially involved effector mechanisms. The innate immune system is a complex nonlinear system orchestrating the coordination of multiple cell types (Lynn et al., 2010), thus *in vivo* studies in cattle and sheep on early *N. caninum* infections are needed to confirm these findings. In fact, it is important to point out that triggers and consequences of the NETotic process *in vivo* are yet not completely understood (Malachowa et al., 2016).

To summarize, we present novel data on ovine NET formation against *N. caninum* tachyzoites and show that parasite exposure leads to both glycolytic and oxidative responses in ovine PMN reflecting their activation. Interestingly, the comparative data evidenced a generally weaker parasite-driven *ex vivo* immune response of sheep compared to cattle. However, further studies with complementary *ex vivo* techniques or using *ex vivo*-derived tissue samples [i.e. placentomes, central nervous system (CNS) or fetal tissues] from infected animals would help to better understand the role of PMN and NETosis in host ruminant susceptibility to *N. caninum* infections.

CRediT authorship contribution statement

D. Gutiérrez-Expósito: Writing – review & editing, Methodology. **L. M. R.Silva:** Writing – review & editing. **H. Wagner:** Writing – review & editing. **A. Taubert:** Writing – review & editing, Supervision. **U. Gärtner:** Writing – review & editing, Methodology. **Conejeros I:** Writing – review & editing, Methodology. **C. Hermosilla:** Writing – review & editing, Methodology.

Funding

DGE has been financially supported by the Ministry of Universities of Spain (MCIN) (Grant “Ayuda para la Recualificación del Profesorado”) and, as appropriate, by “European Union NextGenerationEU/PRTR”.

Declaration of Competing Interest

The authors declare that they have no known competing financial interests or personal relationships that could have appeared to influence the work reported in this paper.

Acknowledgement

The authors would like to acknowledge all staff members of the Institute for Parasitology, JLU Giessen, especially Dr. Christine Ritter and Hannah Salecker for their excellent technical assistance. The authors extend their gratitude to the personnel affiliated to the Oberer Hardthof Livestock Teaching and Research Facility (JLU Giessen). Finally, we thank Anika Seipp of the Institute of Anatomy and Cell Biology (JLU Giessen) for her excellent technical assistance in SEM analysis.

Appendix A. Supporting information

Supplementary data associated with this article can be found in the online version at doi:10.1016/j.vetpar.2026.110797.

References

Abi Abdallah, D.S., Lin, C., Ball, C.J., King, M.R., Duhamel, G.E., Denkers, E.Y., 2012. *Toxoplasma gondii* triggers release of human and mouse neutrophil extracellular traps. Infect. Immun. 80, 768–777. https://doi.org/10.1128/iai.05730-11.

Almyroudis, N.G., Grimm, M.J., Davidson, B.A., Rohm, M., Urban, C.F., Segal, B.H., 2013. NETosis and NADPH oxidase: at the intersection of host defense, inflammation and injury. Front Immunol. 4, 45. https://doi.org/10.3389/fimmu.2013.00045.

Arteche-Villasol, N., Gutiérrez-Expósito, D., Criado, M., Benavides, J., Pérez, V., 2022. Assessment of paratuberculosis vaccination effect on *in vitro* formation of neutrophil extracellular traps in a sheep model. Vaccines 10, 1403. https://doi.org/10.3390/vaccines10091403.

Baker, V.S., Imade, G.E., Molta, N.B., Tawde, P., Pam, S.D., Obadofin, M.O., Sagay, S.A., Egah, D.Z., Iya, D., Afolabi, B.B., Baker, M., Ford, K., Ford, R., Roux, K.H., Keller III, T.C., 2008. Cytokine-associated neutrophil extracellular traps and antinuclear antibodies in *Plasmodium falciparum* infected children under six years of age. Malar. J. 7, 41. https://doi.org/10.1186/1475-2875-7-41.

Behrendt, J.H., Ruiz, A., Zahner, H., Taubert, A., Hermosilla, C., 2010. Neutrophil extracellular trap formation as innate immune reactions against the apicomplexan parasite *Eimeria bovis*. Vet. Immun. Immunopathol. 133, 1–8. https://doi.org/10.1016/j.vetimm.2009.06.012.

Benavides, J., González-Warleta, M., Arteche-Villasol, N., Pérez, V., Mezo, M., Gutiérrez-Expósito, D., 2022. Ovine neosporosis: the current global situation. Anim. 12, 2074. https://doi.org/10.3390/ani12162074.

Bliss, S.K., Gavrilescu, C., Alcaraz, A., Denkers, E.Y., 2001. Neutrophil depletion during *Toxoplasma gondii* infection leads to impaired immunity and lethal systemic pathology. Infect. Immun. 69, 4898–4905. https://doi.org/10.1128/IAI.69.8.4898-4905.2001.

Bondurant, R.H., 1999. Inflammation in the bovine female reproductive tract. J. Anim. Sci. 77, 101–110. https://doi.org/10.2527/1999.77suppl_2101x.

Boysen, P., Olsen, I., Berg, I., Kulberg, S., Johansen, G.M., Storset, A.K., 2006. Bovine CD2-/NKp46+ cells are fully functional natural killer cells with a high activation status. BMC Immunol. 7, 10. https://doi.org/10.1186/1471-2172-7-10.

Brinkmann, V., Reichard, U., Goosmann, C., Fauler, B., Uhlemann, Y., Weiss, D., Weinrauch, Y., Zychlinsky, A., 2004. Neutrophil extracellular traps kill bacteria. Science 303, 1532–1535. https://doi.org/10.1126/science.1092385.

Brinkmann, V., Goosmann, C., Kuhn, L., Zychlinsky, A., 2013. Automatic quantification of *in vitro* NET formation. Front. Inmmunol 3, 413. https://doi.org/10.3389/fimmu.2012.00413.

Brinkmann, V., Abu-Abed, U., Goosmann, C., Zychlinsky, A., 2016. Immunodetection of NETs in paraffin-embedded tissue. Front Immunol. 7, 513. https://doi.org/10.3389/fimmu.2016.00513.

Brown, L., Yipp, B., 2023. Neutrophil swarming: is a good offense the best defense? iScience 26, 107655. https://doi.org/10.1016/j.isci.2023.107655.

Burgos, R.A., Werling, D., Hermosilla, C., 2022. Editorial: The emerging role of metabolism and metabolic-related receptors on neutrophil extracellular traps (NET) formation. Front Immunol. 13, 1028228. https://doi.org/10.3389/fimmu.2022.1028228.

Buxton, D., McAllister, M.M., Dubey, J.P., 2002. The comparative pathogenesis of neosporosis. Trends Parasitol. 18 (12), 546–552. https://doi.org/10.1016/s1471-4922(02)02414-5.

Castanheira, F.V.S., Kubes, P., 2019. Neutrophils and NETs in modulating acute and chronic inflammation. Blood 133, 2178–2185. https://doi.org/10.1182/blood-2018-11-844530.

Chacko, B.K., Kramer, P.A., Ravi, S., Johnson, M.S., Hardy, R.W., Ballinger, S.W., Darley-Usmar, V.M., 2013. Methods for defining distinct bioenergetic profiles in platelets,

lymphocytes, monocytes, and neutrophils, and the oxidative burst from human blood. Lab Invest 93, 690–700. https://doi.org/10.1038/labinvest.2013.53.
Conejeros, I., López-Osorio, S., Zhou, E., Velásquez, Z.D., Del Río, M.C., Burgos, R.A., Alarcón, P., Chaparro-Gutiérrez, J.J., Hermosilla, C., Taubert, A., 2022. Glycolysis, monocarboxylate transport, and purinergic signaling are key events in *Eimeria bovis*-induced NETosis. Front Immunol. 13, 842482. https://doi.org/10.3389/fimmu.2022.842482.
Demattio, L., Conejeros, I., Grob, D., Gartner, U., Taubert, A., Hermosilla, C., Wehrend, A., 2023. Induction of NETosis in ovine colostral PMN upon exposure to *Neospora caninum* tachyzoites. Front Vet. Sci. 10, 1176144. https://doi.org/10.3389/fvets.2023.1176144.
Dubey, J.P., 1986. A review of toxoplasmosis in cattle. Vet. Parasitol. 22, 177–202. https://doi.org/10.1016/0304-4017(86)90106-8.
Dubey, J.P., Hattel, A.L., Lindsay, D.S., Topper, M.J., 1988. Neonatal *Neospora caninum* infection in dogs: isolation of the causative agent and experimental transmission. J. Am. Vet. Med. Assoc. 193 (10), 1259–1263. https://doi.org/10.2460/javma.1988.193.10.1259.
Dubey, J.P., Schares, G., Ortega-Mora, L.M., 2007. Epidemiology and control of neosporosis and *Neospora caninum*. Clin. Microbiol. Rev. 20, 323–367. https://doi.org/10.1128/CMR.00031-06.
Espinosa, G., Conejeros, I., Rojas-Barón, L., Hermosilla, C.R., Taubert, A., 2023. *Besnoitia besnoiti*-induced neutrophil clustering and neutrophil extracelular trap formation depend on P2X1 purinergic receptor signaling. Front Immunol. 14, 1244068. https://doi.org/10.3389/fimmu.2023.1244068.
Euler, M., Hoffmann, M.H., 2019. The double-edged role of neutrophil extracellular traps in inflammation. Biochem. Soc. Trans. 47, 1921–1930. https://doi.org/10.1042/BST20190629.
Fonseca, Z., Díaz-Godínez, C., Mora, N., Aleman, O.R., Uribe-Querol, E., Carrero, J.C., Rosales, C., 2018. *Entamoeba histolytica* induce signaling via Raf/MEK/ERK for neutrophil extracellular trap (NET) formation. Front Cell Infect. Microbiol. 8, 226. https://doi.org/10.3389/fcimb.2018.00226.
García-Sánchez, M., Jiménez-Pelayo, L., Vázquez, P., Horcajo, P., Regidor-Cerrillo, J., Jiménez-Meléndez, A., Osoro, K., Ortega-Mora, L.M., Collantes-Fernández, E., 2021. Maternal and foetal celular immune responses in dams infected with high- and low-virulence isolates of *Neospora caninum* at mid-gestation. Front Cell Infect. Microbiol. 11, 684670. https://doi.org/10.3389/fcimb.2021.684670.
Garza, J.J., Greiner, S.P., Bowdridge, S.A., 2018. Ovine vital neutrophil extracellular traps bind and impair *Haemonchus contortus* L3 in a breed-dependent manner. Parasite Immunol. 40, 12572. https://doi.org/10.1111/pim.12572.
Gilbert, R.O., Shin, S.T., Guard, C.L., Erb, N.H., Frajblat, M., 2005. Prevalence of endometritis and its effects on reproductive performance of dairy cows. Theriogenology 64 (9), 1879–1888. https://doi.org/10.1016/j.theriogenology.2005.04.022.
González-Warleta, M., Castro-Hermida, J.A., Calvo, C., Pérez, V., Gutiérrez-Expósito, D., Regidor-Cerrillo, J., Ortega-Mora, L.M., Mezo, M., 2018. Endogenous transplacental transmisión of *Neospora caninum* during successive pregnancies across three generations of naturally infected sheep. Vet. Res. 19 (1), 106. https://doi.org/10.1186/s13567-018-0601-3.
Grob, D., Conejeros, I., Velásquez, Z.D., Preusser, C., Gartner, U., Alarcon, P., Burgos, R. A., Hermosilla, C., Taubert, A., 2020. *Trypanosoma brucei brucei* induces polymorphonuclear neutrophil activation and neutrophil extracellular traps release. Front Immunol. 22, 559561. https://doi.org/10.3389/fimmu.2020.559561.
Grudzinska, F.S., Jasper, A., Sapey, E., Thickett, D.R., Mauro, C., Scott, A., Barlow, J., 2023. Real-time assessment of neutrophil metabolism and oxidative burst using extracellular flux analysis. Front Immunol. 14, 1083072. https://doi.org/10.3389/fimmu.2023.1083072.
Hasheminasab, S.S., Conejeros, I., Velásquez, Z., Borggrefe, T., Gartner, U., Kamena, F., Taubert, A., Hermosilla, C., 2022. ATP purinergic recepctor P2X1-dependant suicidal NETosis induced by *Cryptosporidirum parvum* under physioxia conditions. Biology 11, 422. https://doi.org/10.3390/biology11030442.
Hakkim, A., Fuchs, T.A., Martínez, N.E., Hess, S., Prinz, H., Zychlinsky, A., Waldmann, H., 2011. Activation of the Raf-MEK-ERK pathway is required for neutrophil extracellular trap formation. Nat. Chem. Biol. 7, 75–77. https://doi.org/10.1038/nchembio.496.
Hermosilla, C., Muñoz-Caro, T., Silva, L.M.R., Ruiz, A., Taubert, A., 2014. The intriguing host innate immune response: novel anti-parasitic defence by neutrophil extracellular traps. Parasitology 141, 1489–1498. https://doi.org/10.1017/S0031182014000316.
Huang, J., Hong, W., Wan, M., Zheng, L., 2022. Molecular mechanisms and therapeutic target of NETosis in diseases. MedComm 3 (3), e162. https://doi.org/10.1002/mco2.162.
Innes, E.A., Bartely, P.M., Maley, S.W., Wright, S.E., Buxton, D., 2007. Comparative host-parasite relationships in ovine toxoplasmosis and bovine neosporosis and strategies for vaccination. Vaccine 25, 5495–5503. https://doi.org/10.1016/j.vaccine.2007.02.044.
Kaplan, M.J., Radic, M., 2012. Neutrophil extracellular traps: double-edged swords of innate immunity. J. Immunol. 13, 922377. https://doi.org/10.4049/jimmunol.1201719.
Klinke, M., Chaaban, H., Boettcher, M., 2023. The role of neutrophil extracellular traps in necrotizing enterocolitis. Front Pedia 11, 1121193. https://doi.org/10.3389/fped.2023.1121193.
Lacy, P., 2006. Mechanisms of degranulation in neutrophils. Allergy Asthma Clin. Immunol. 2, 98–108. https://doi.org/10.1186/1710-1492-2-3-98.
Ladero-Auñon, I., Molina, E., Holder, A., Kolakowski, J., Harris, H., Urkitza, A., Anguita, J., Werling, D., Elguezabal, N., 2021. Bovine neutrophils release extracellular traps and cooperate with macrophages in *Mycobacterium avium* subsp. *paratuberculosis* clearance *in vitro*. Front. Immunol. 12, 645304. https://doi.org/10.3389/fimmu.2021.645304.
Lee, W.L., Harrison, R.E., Grinstein, S., 2003. Phagocytosis by neutrophils. Microbes Infect. 5, 1299–1306. https://doi.org/10.1016/j.micinf.2003.09.014.
Lynn, D.J., Chan, C., Naseer, M., Yau, M., Lo, R., Sribnaia, A., Ring, G., Que, J., Wee, K., Winsor, G.L., Laird, M.R., Breuer, K., Foroushani, A.K., Brinkman, F.S.L., Hancock, R. E.W., 2010. Curating the innate immunity interactome. BMC Syst. Biol. 4, 117. https://doi.org/10.1186/1752-0509-4-117.
Malachowa, N., Kobayashi, S.D., Quinn, M.T., DeLeo, F.R., 2016. NET confusion. Front Immunol. 7, 259. https://doi.org/10.3389/fimmu.2016.00259.
Mendoza-Morales, L.F., Lagorio, V., Corigliano, M.G., Sánchez-López, E., Ramos-Duarte, V.A., Clemente, M., Sander, V.A., 2022. Neosporosis in sheep: a systematic review and meta-analysis of global seroprevalence and related risk factors. Acta Trop. 233, 106569. https://doi.org/10.1016/j.actatropica.2022.106569.
Mohammed, S., Alhussien, M.N., Dang, A.K., 2022. Pregnancy stage-dependent modulation of neutrophil function may impact embryo survivability and pregnancy outcome in crossbred cows. Theriogenology 191, 200–206. https://doi.org/10.1016/j.theriogenology.2022.08.020.
Muñoz-Caro, T., Hermosilla, C., Silva, L.M.R., Cortes, H., Taubert, A., 2014. Neutrophil extracelular traps as innate immune reaction against the emerging apicomplexan parasite *Besnoitia besnoiti*. Plos One 9, e91415. https://doi.org/10.1371/journal.pone.0091415.
Muñoz-Caro, T., Mena-Huertas, S.J., Conejeros, I., Alarcón, P., Hidalgo, M.A., Burgos, R. A., Hermosilla, C., Taubert, A., 2015a. *Eimeria bovis*-triggered neutrophil extracellular trap formation is CD11b-, ERK1/2-, p38 MAP kinase and SOCE-dependent. Vet. Res. 46, 23. https://doi.org/10.1186/s13567-015-0155-6.
Muñoz-Caro, T., Lendner, M., Daugschies, A., Hermosilla, C., Taubert, A., 2015b. NADPH oxidase, MPO, NE, ERK1/2, p38 MAPK and Ca2+ influx are essential for *Cryptosporidium parvum*-induced NET formation. Dev. Comp. Immunol. 52, 245–254. https://doi.org/10.1016/j.dci.2015.05.007.
Muñoz-Caro, T., Silva, L.M.R., Rentería-Solís, Z., Taubert, A., Hermosilla, C., 2016. Neutrophil extracelular traps in the intestinal mucosa of *Eimeria*-infected animals. Asian Pac. J. Trop. Biomed. 6, 301–307. https://doi.org/10.1016/j.apjtb.2016.01.001.
Nauseef, W.M., 2007. How human neutrophils kill and degrade microbes: an integrated view. Immunol. Rev. 219, 88–102. https://doi.org/10.1111/j.1600-065X.2007.00550.x.
Nauseef, W.M., 2023. Humand neutrophils ≠ murine neutrophils: does it matter? Immunol. Rev. 314, 442–456. https://doi.org/10.1111/imr.13154.
Quiroga, J., Alarcón, P., Ramírez, M.F., Manosalva, C., Teuber, S., Carretta, M.D., Burgos, R.A., 2023. D-lactate-induced ETosis in cattle polymorphonuclear leucocytes in dependent on the release of mitochondrial reactive oxygen species and the PI3K/Akt/HIF-1 and GSK-3β pathways. Dev. Comp. Immunol. 145, 104728. https://doi.org/10.1016/j.dci.2023.104728.
Ravindran, M., Khan, M.A., Palaniyar, N., 2019. Neutrophil extracellular trap formation: physiology, pathology, and pharmacology. Biomolecules 9, 365. https://doi.org/10.3390/biom9080365.
Regidor-Cerrillo, J., Gómez-Bautista, M., Pereira-Bueno, J., Aduriz, G., Navarro-Lozano, V., Risco-Castillo, V., Fernández-García, A., Pedraza-Díaz, S., Ortega-Mora, L.M., 2008. Isolation and genetic characterization of *Neospora caninum* from asymptomatic calves in Spain. Parasitology 135, 1651–1659. https://doi.org/10.1017/S003118200800509X.
Rinaldi, M., Moroni, P., Paape, M.J., Bannerman, D.D., 2007. Evaluation of assays for the measurement of bovine neutrophil reactive oxygen species. Vet. Immunol. Immunopathol. 115, 107–125. https://doi.org/10.1016/j.vetimm.2006.09.009.
Schindelin, J., Arganda-Carreras, I., Erwin, F., Kaynig, V., Longair, M., Pietzsch, T., Preibisch, S., Rueden, C., Saalfeld, S., Schmid, B., Tinevez, J.Y., White, D.J., Hartenstein, V., Eliceiri, K., Tomancak, P., Cardona, A., 2012. Fiji: an open-source platform for biological-image analysis. Nat. Methods 9, 676–682. https://doi.org/10.1038/nmeth.2019.
Sharma, P., Hartley, C.S., Haque, M., Coffey, T.J., Sharon, A.E., Flynn, R.J., 2018. Bovine neonatal monocytes display phenotypic differences compared with adults after challenge with the infectious abortifacient agent *Neospora caninum*. Front Immunol. 9, 3011. https://doi.org/10.3389/fimmu.2018.03011.
Silva, L.M.R., Caro, T.M., Gerstberger, R., Vila-Vicosa, M.J.M., Cortés, H., Hermosilla, C., 2014. *Eimeria arloingi* induces caprine neutrophil extracelular traps. Parasitol. Res. 113, 2797–2807. https://doi.org/10.1007/s00436-014-3939-0.
Swain, D.K., Kushwah, M.S., Kaur, M., Patbandha, T.K., Monhanty, A.K., Dang, A., 2014. Formation of NET, phagocytic activity, surface architecture, apoptosis and expression of toll like receptors 2 and 4 (TLR2 and TLR4) in neutrophils of mastitic cows. Vet. Res. Commun. 38, 209–219. https://doi.org/10.1007/s11259-014-9606-1.
Taubert, A., Krull, M., Zahner, H., Hermosilla, C., 2006. *Toxoplasma gondii* and *Neospora caninum* infections of bovine endothelial cells induce endothelial adhesion molecule gene transcription and subsequent PMN adhesion. Vet. Immunol. Immunopathol. 112, 272–283. https://doi.org/10.1016/j.vetimm.2006.03.017.
Thiam, H.R., Wong, S.L., Wagner, D.D., Waterman, C.M., 2020. Cellular mechanisms of NETosis. Annu Rev. Cell Dev. Biol. 36, 191–2018. https://doi.org/10.1146/annurev-cellbio-020520-111016.
Villagra- Blanco, R., Silva, L.M.R., Muñoz-Caro, T., Yang, Z., Li, J., Gartner, U., Taubert, A., Zhang, X., Hermosilla, C., 2017a. Bov. Polymorphonucl. neutrophils Cast. neutrophil Extracell. traps Abort. Parasite Neospora caninum. https://doi.org/10.3389/fimmu.2017.00606.
Villagra-Blanco, R., Silva, L.M.R., Gartner, U., Wagner, H., Failing, K., Wehrend, A., Taubert, A., Hermosilla, C., 2017b. Molecular analysis on *Neospora caninum*-

triggered NETosis in the caprine system. Dev. Comp. Immunol. 72, 119–127. https://doi.org/10.1016/j.dci.2017.02.020.
Worku, M., Rehrah, D., Ismail, H.D., Asiamah, E., Adjei-Fremah, S., 2021. A review of the neutrophil extracellular traps (NETs) from cow, sheep and goat models. Int. J. Mol. Sci. 22, 8046. https://doi.org/10.3390/ijms22158046.
Yildiz, K., Gokpinar, S., Gazyagci, A.N., Babur, C., Sursal, N., Azkur, A.K., 2017. Role of NETs in the difference in host susceptibility to *Toxoplasma gondii* between sheep and cattle. Vet. Immunol. Immunopathol. 189, 1–10. https://doi.org/10.1016/j.vetimm.2017.05.005.
Zamboni, D.S., Lima-Junior, D.S., 2015. Inflammasomes in host response to protozoan parasites. Immunol. Rev. 265, 156–171. https://doi.org/10.1111/imr.12291.
Zhang, J., Sun, Y., Zheng, J., 2021. The state of art of extracellular traps in protozoan infections (review). Fron Immunol. 12, 770246. https://doi.org/10.3389/fimmu.2021.770246.